

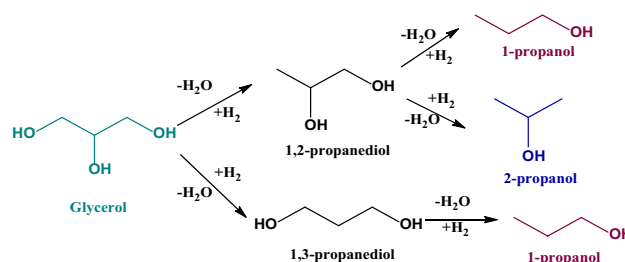
Direct Hydrogenolysis of Glycerol to Biopropanols over Metal Phosphate Supported Platinum Catalysts

Ponnala Bhanuchander¹ · Samudrala Shanthi Priya^{1,2} · Vanama Pavan Kumar¹ · Sk. Hussain¹ · N. Pethan Rajan¹ · Suresh K. Bhargava² · Komandur V. R. Chary¹

Received: 26 September 2016 / Accepted: 20 December 2016 / Published online: 28 February 2017
© Springer Science+Business Media New York 2017

Abstract Several metal phosphate supported platinum catalysts (Pt/AlP, Pt/TiP, Pt/ZrP and Pt/NbP) have been synthesized for the direct hydrogenolysis of glycerol to produce bio-propanols performed under mild reaction conditions. The catalysts were screened for its activity towards production of propanols from glycerol hydrogenolysis and the reaction has been optimized by studying various reaction parameters such as effect of platinum loading, reaction temperature, hydrogen flow rate, glycerol concentration and reaction time. Among the catalysts investigated, 2Pt/TiP presented a remarkable catalytic performance for vapour phase hydrogenolysis of glycerol with 100% conversion of glycerol and 97% selectivity to total propanols (1-propanol + 2-propanol) at 220 °C and atmospheric pressure. The high efficiency of 2Pt/TiP catalyst is probably be due to the strong acidity of catalyst and the uniform dispersion of small Pt particles on surface of TiP that could enable the dehydration-hydrogenation route of glycerol hydrogenolysis. Further, the structural characteristics of used catalyst have been investigated in order to understand the stability of the catalyst. Therefore, a more economical and sustainable approach of producing value added propanols from bio-derived glycerol over highly efficient catalytic system is herein presented.

Graphical Abstract



Keywords Biopropanols · Hydrogenolysis · Metal phosphates · Glycerol · Platinum catalysts

1 Introduction

The use of biomass as a sustainable feedstock for the production of chemicals and fuels has received significant interest in recent years due to wide availability and renewability. Biodiesel is among one of the promising fuel, and it is produced by transesterification of vegetable oils with methanol under basic conditions [1]. It is also considered to be the attractive alternative to the fossil fuel energy resources. Glycerol is a major byproduct of biodiesel production and it becomes very important molecule in the aspects of renewable biomass resources. Hence, much attention has been paid on the conversion of biomass derived glycerol to value added chemicals such as acrolein, acrylic acid, glyceric acid, 1,2-propanediol, 1,3-propanediol etc [2–6]. Continuous synthesis of 1,2-PDO, 1,3-PDO and propanols from biomass derived glycerol via hydrogenolysis process under ambient condition is an important process in the industrial point of view because of various uses of these products in the synthesis of polyester resins,

✉ Komandur V. R. Chary
kvrchary@iict.res.in

¹ Inorganic and Physical Chemistry Division, CSIR-Indian Institute of Chemical Technology, Uppal Road, Hyderabad 500007, India

² Centre for Advanced Materials & Industrial Chemistry (CAMIC), School of Applied Sciences, RMIT University, GPO BOX 2476, Melbourne 3001, Australia

detergents, flavoring agents, cosmetics, pharmaceuticals, paints, etc [7–10]. However, bio-propanols such as 1-propanol and 2-propanol are also important commodity chemicals with significant applications. Hence, synthesis of these bio-propanols from glycerol is an attractive route because this process is renewable one and also alternative to the available petrochemical process. Presently, 1-propanol, and 2-propanol are prepared from the hydroformylation of ethylene and hydration of propylene respectively [11, 12].

Zhu et al. reported the one-step hydrogenolysis of biomass-derived glycerol to propanols over different supported Pt–H₄SiW₁₂O₄₀ (HSiW) bi-functional catalysts in aqueous media and they obtained yield of 94% of propanols [13]. Lin et al. studied hydrogenolysis of glycerol in a sequential two-layer bed system in a continuous-flow fixed-bed reactor with H-β zeolite and Ni/Al₂O₃ catalysts. This two bed catalytic system afforded 1-propanol selectively (69%) with maximum glycerol conversion (~100%) [14]. Tamura et al. studied the promoting effect of Ru over Ir–ReOx/SiO₂ catalyst for the selective hydrogenolysis of glycerol and they found that Ru promoted Ir–ReOx/SiO₂ catalyst was efficient catalyst for the production of 1,3-propanediol and 1-propanol [15]. Recently, our group also reported metal-acid bifunctional catalysts containing platinum and different heteropolyacids (HPA) supported on zirconia for the hydrogenolysis of glycerol under normal atmospheric pressure and we obtained excellent yield (98%) of propanols over Pt–PTA/ZrO₂ at 230°C [16]. Very recently, Wang et al. investigated hydrogenolysis of glycerol to 1-propanol by a two layer catalytic system containing zirconium phosphate and supported Ru catalysts [17]. Despite of various research efforts made earlier, it is still necessary to find an efficient catalytic system in order to meet practical demands of propanol production in terms of its selectivity, catalyst stability and environmental friendly conditions.

Glycerol hydrogenolysis proceeds through a dehydration-hydrogenation route as reported in the previous studies [18, 19]. Initially, the glycerol undergoes dehydration-hydrogenation over acid and metal sites of the catalyst to

give 1,2-propanediol and 1,3-propanediol respectively. The propanediols thus produced undergoes further dehydration-hydrogenation over the metal-acid catalyst to give 1-propanol and 2-propanol respectively (Scheme 1). Therefore, a highly efficient and selective catalytic system is vital to perform direct hydrogenolysis of glycerol to propanols in a single step.

Herein, we report here the hydrogenation of glycerol to bio-propanols under ambient condition and continuous process over a platinum catalyst supported on various metal phosphates as supports (ZrP, TiP, NbP and AIP). The catalysts were prepared by wet impregnation method and characterized by XRD analysis, BET surface area, NH₃-temperature programmed desorption (NH₃-TPD), Pyridine adsorbed Fourier Transform Spectroscopy (Py-FTIR), Transmission electron microscopy (TEM) and CO pulse chemisorption. The purpose of this work is to screen out the highly efficient catalyst for the reaction and to understand the catalytic properties responsible for the good catalytic activity during the hydrogenation of glycerol to bio-propanols.

2 Experimental

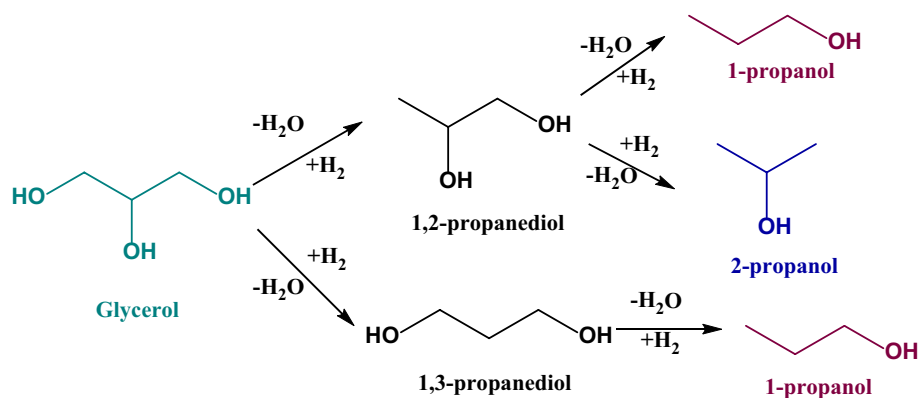
2.1 Catalyst Preparation

2.1.1 Preparation of Metal Phosphates

The different metal phosphates such as Aluminum phosphate, Titanium phosphate, Zirconium phosphate, and Niobium phosphates were used as support materials in the present study and are prepared by following the previously reported procedures [6, 7].

Preparation of Aluminium phosphate A hydrothermal method of synthesizing amorphous aluminium phosphate (AIP) was employed [20] in which aluminium nitrate [Al(NO₃)₃·6H₂O] and diammonium hydrogen phosphate [(NH₄)₂HPO₄] were used as precursor materials.

Scheme 1 Hydrogenolysis of glycerol to produce propanols



The required amounts of aluminium and phosphorous precursors (P/Al ratio of 0.9) were dissolved in water under constant stirring and then acidified with nitric acid. The pH of the solution was adjusted to 8 by addition of aqueous ammonia. After 1 h of continuous stirring, the hydrogel thus obtained was filtered, washed with distilled water to remove excess solvent and dried overnight at 110 °C followed by calcinations in air for 30 min at 500 °C.

Preparation of Titanium Phosphate In a typical hydrothermal process [21], Titanium phosphate (TiP) was synthesized by using a mixture of titanium *n*-butoxide (TBT) and *n*-butanol to which 30 mL of 0.1 M phosphoric acid solution was added drop wise and kept under stirring for 2 h at room temperature. The mixture obtained was aged for 24 h at 80 °C in a Teflon-lined autoclave. The product was then filtered, washed with water, dried at 60 °C for 12 h and finally calcined at 500 °C for 2 h.

Preparation of Zirconium Phosphate Zirconium phosphate (ZrP) was prepared by adding 0.01 mol of Zirconium *n*-propoxide (70 wt% solution in 1-propanol, Aldrich) to a solution of 85% phosphoric acid (60 mL of 0.1 mol L⁻¹) under stirring at room temperature. The mixture obtained after 2 h of stirring was transferred into a Teflon lined autoclave and aged at 80 °C for 24 h. The final product was filtered, dried and calcined at 400 °C for 5 h [22].

Preparation of Niobium Phosphate The NbP catalyst was synthesized by the procedure reported elsewhere [23]. In a typical procedure, 2.73 g of NbCl₅ was dissolved in 50 mL of H₂O and 2.30 g of H₃PO₄ (Aldrich, 85% aqueous solution) was added followed by an additional 50 mL of H₂O. The reaction mixture was allowed to stir for 30 min by maintaining the pH of the solution to 2.60 with aqueous ammonia. The resulting slurry was filtered and washed by deionised water. The obtained gel then was mixed with 10 mL of H₂O and 1.45 g of hexadecylamine and stirred for 30 min. About 0.92 g H₃PO₄ (85%) was added to the above solution and the pH was adjusted to 3.88 by adding ammonia solution. The formed slurry was heated in a Teflon-lined autoclave and aged statically at 110 °C for 48 h. The final product was filtered, washed with deionised water, dried 100 °C overnight, and subsequently calcined at 550 °C in air for 6 h.

2.1.2 Preparation of Supported Platinum Catalysts

The metal phosphate supported platinum catalysts were prepared by wet impregnation method. An aqueous solution of H₂PtCl₆·6H₂O was impregnated with required amounts of different metal phosphates individually under vigorous stirring. After the excess amount of water is lost, the impregnated sample was allowed to dry overnight at 110 °C and the resulting material was calcined at 450 °C for 3 h. The platinum loading in all the catalysts is fixed to 2 wt%

and the catalysts are hereafter notated as 2Pt/AlP, 2Pt/TiP, 2Pt/ZrP and 2Pt/NbP in the following discussion. In addition, a series of platinum catalysts supported on TiP with different platinum loadings (0.5–3 wt%) were prepared by following the same procedure.

2.2 Catalyst Characterization

X-ray diffraction (XRD) analysis of the fresh and used catalysts were performed in the 2θ range of 2° to 65°, on Rigaku miniflex X-ray diffractometer at a scan rate of 2°/min with the beam voltage and a beam current of 30 kV and 15 mA respectively.

The textural properties such as surface area, pore volume and pore diameter of the catalysts were analyzed using N₂-adsorption at -196 °C by the multipoint BET method on Autosorb 1 (Quantachrome instruments, USA).

TPD experiments were carried out on AutoChem 2910 (Micromeritics, USA) instrument. In a typical experiment, 100 mg of oven dried sample was pretreated by passage of high purity (99.995%) helium (50 mL/min) at 200 °C for 1 h. After pretreatment, the sample was saturated with highly pure anhydrous ammonia (50 mL/min) with a mixture of 10% NH₃-He at 80 °C for 1 h and subsequently flushed with He flow (50 mL/min) at 80 °C for 30 min to remove physisorbed ammonia. TPD analysis was carried out from ambient temperature to 600 °C at a heating rate of 10 °C/min. The amount of NH₃ desorbed was calculated using GRAMS/32 software.

The investigation of nature of acid sites was analyzed by pyridine adsorption on the catalysts followed by FTIR experiments. The FTIR spectra of the samples were taken on the IR (Model: GC-FT-IR Nicolet 670) spectrometer by KBr disc method under ambient condition.

CO-chemisorption measurements were carried out on AutoChem 2910 (Micromeritics, USA) instrument. Prior to adsorption measurements, ca. 100 mg of the sample was reduced in a flow of hydrogen (50 mL/min) at 400 °C for 3 h and flushed out subsequently in a pure helium gas flow for an hour at 400 °C. The sample was subsequently cooled to ambient temperature in the same He stream. CO uptake was determined by injecting pulses of 9.96% CO balanced helium from a calibrated on-line sampling valve into the helium stream passing over the reduced samples at 400 °C. Platinum surface area, percentage dispersion and Pt average particle size were calculated assuming the stoichiometric factor (CO/Pt) as 1. Adsorption was deemed to be complete after three successive runs showed similar peak areas.

2.3 Catalyst Testing

The vapour phase hydrogenolysis of glycerol was carried out in a vertical fixed bed quartz reactor (40 cm length,

9 mm i.d.) under atmospheric pressure. Prior to the reaction, the 0.5 g of catalysts were pretreated at 350 °C for 2 h in flowing H₂ (80 mL/min). After cooling down to the reaction temperature (220 °C), hydrogen (100 mL/min) and an aqueous solution of 10 wt% glycerol were introduced into the reactor through a heated evaporator. The reaction products were condensed in an ice–water trap and collected hourly for analysis on a gas chromatograph GC-2014(Shimadzu) equipped with a DB-wax 123-7033 (Agilent) capillary column (0.32 mm i.d., 30 m long) and equipped with flame ionization detector. The conversion of glycerol and selectivity of products were calculated as follows:

$$\text{Conversion(\%)} = \frac{\text{moles of glycerol (in)} - \text{moles of glycerol (out)}}{\text{moles of glycerol (in)}} \times 100$$

$$\text{Selectivity (\%)} = \frac{\text{moles of one product}}{\text{moles of all products}} \times 100$$

3 Results and Discussion

3.1 Characterization Techniques

3.1.1 X-ray Diffraction (XRD)

The X-ray diffraction studies of pure metal phosphates and metal phosphate supported platinum catalysts (2Pt/AiP, 2Pt/TiP, 2Pt/ZrP and 2Pt/NbP) were carried out and the diffraction patterns are presented in Fig. 1. All the synthesized metal phosphates were found to be X-ray amorphous as

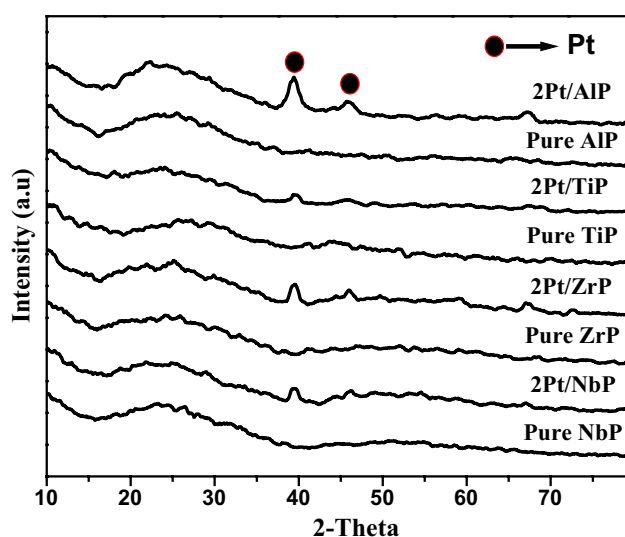


Fig. 1 XRD patterns of pure metal phosphates and platinum catalysts

suggested from the XRD results. In addition, small peaks at $2\theta = 39.7^\circ$ and 46.1° coinciding with (111) and (200) lattice planes of platinum are observed in metal phosphate supported platinum catalysts. However, the intensity of Pt peak is different in different metal phosphate supported platinum catalysts. In comparison to other catalysts, 2Pt/TiP catalyst reveals the presence of very less intense Pt peak indicating the fine dispersion of Pt on surface of TiP.

3.1.2 Temperature Programmed Desorption of Ammonia (NH₃-TPD)

The total acidity and the strength of acid sites in various

metal phosphate supported platinum catalysts was determined by the ammonia temperature programmed desorption technique. The desorption of ammonia in the temperature range 50–250 °C, 250–350 and > 350 °C corresponds to the presence of weak, moderate and strong acid sites respectively [24]. The NH₃-TPD profiles and the total acidity ($\mu\text{mol/g}$ calculated from area under the peaks) of all the metal phosphate supported platinum catalysts are shown in Fig. 2 and Table 1. The ammonia adsorption–desorption technique usually enables determination of the strength of acid sites present on the catalyst surface together with total acidity. It is observed that 2Pt/AiP, 2Pt/ZrP and 2Pt/NbP catalysts possess weak and moderate acid sites with desorption in two different temperature regions.

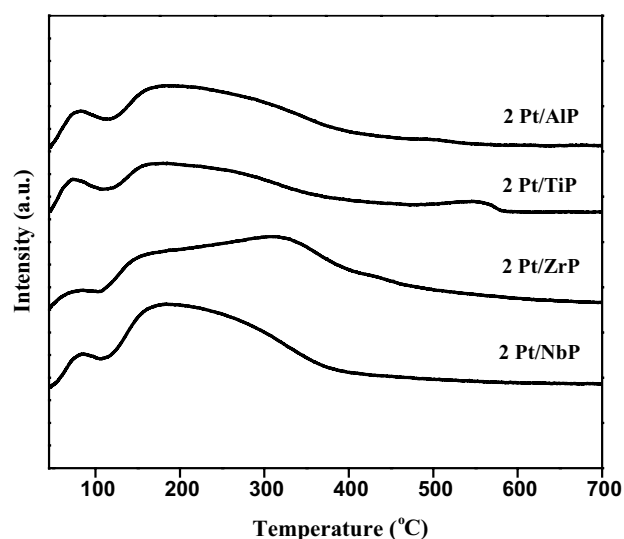


Fig. 2 NH₃-TPD profiles of various metal phosphate supported platinum catalysts

Table 1 Acidities of various metal phosphate supported platinum catalysts

Catalyst	NH ₃ uptake (μmol/g)			Total acidities (μmol/g)
	Weak	Moderate	Strong	
2Pt/AIP	904	58	–	962
2Pt/TiP	145	934	44	1123
2Pt/ZrP	133	1198	–	1331
2Pt/NbP	143	1223	–	1366

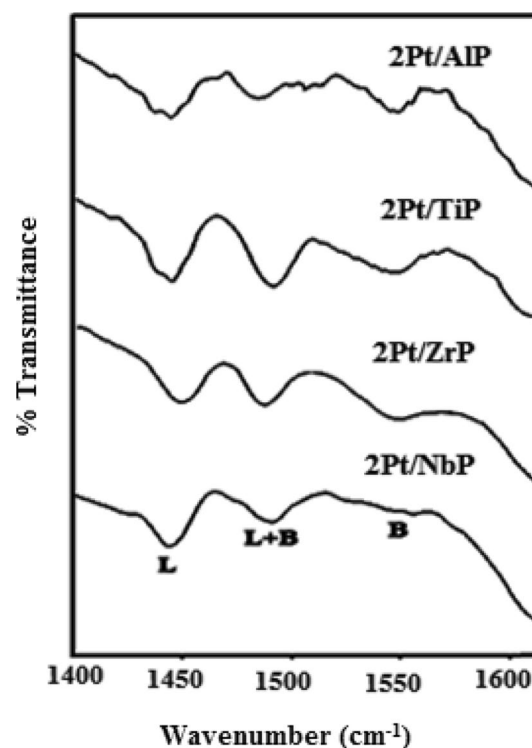
It is interesting to note that, 2Pt/TiP catalyst showed an observable desorption of ammonia in the temperature region > 350 °C indicating the presence of strong acid sites in addition to the presence of weak and moderate acid sites. This might lead to an obvious distinct result in the catalytic activity. However, the total acidity of the catalysts varied and follows the order: 2Pt/NbP > 2Pt/ZrP > 2Pt/TiP > 2Pt/AIP. Therefore, NH₃-TPD is an important technique which enabled to study the acidic strength of catalysts and to further evaluate its role in the catalytic activity.

3.1.3 Pyridine Adsorbed Fourier Transform Infrared Spectroscopy (Pyr-FTIR)

As NH₃-TPD is a useful technique to determine the acidic strength of catalysts, Pyridine adsorbed FTIR technique is another such method used to find the nature/type of acidic sites present in the catalyst. Figure 3 shows the Pyr-FTIR spectra of various metal phosphate supported platinum catalysts in the spectral range of 1400–1600 cm⁻¹. All the samples revealed the presence of three main bands in the spectra. A band at 1453 cm⁻¹ corresponding to the adsorption of pyridine at the Lewis acid sites (L) is clearly observed. On the other hand, a band at 1543 cm⁻¹ due to pyridinium ion on Brønsted acid sites [25] is confirmed which could be attributed to the presence of P(OH) groups in the metal phosphates. However, the intensity of band due to Brønsted acidity varied in each catalyst and was found to be more prominent in 2Pt/AIP catalyst compared to other catalysts. In addition, a band at 1492 cm⁻¹ corresponding to the adsorbed pyridine on both Lewis and Brønsted acid sites was also observed in all the samples.

3.1.4 BET Surface Area

The surface areas of the metal phosphate supported platinum catalysts were determined by using BET method and are listed in Table 2. The deposition of platinum on respective metal phosphate supports led to the significant decrease in the surface area compared to pure metal phosphate supports. This is obvious due to the blockage of pores

**Fig. 3** Pyr-FTIR spectra of various metal phosphate supported platinum catalysts

of metal phosphates by platinum particles. A noticeable decrease in the pore volumes and pore diameters of metal phosphate supported platinum catalysts was also observed. Similar findings were observed in the previous reports [26].

3.1.5 CO-Chemisorption

In order to estimate the dispersion of platinum on various metal phosphate supports, metal surface area and the particle diameter of platinum, CO chemisorption method was employed and the results are tabulated in Table 3. The dispersion of Pt on each metal phosphate support varied and it was found that Pt was highly dispersed (31.1%) on TiP support. The metal surface area of all the catalysts was found to be in the range of 1.06–1.53 m²/g of catalyst whereas the particle size varied between 3.6 and 5.2 nm. Therefore CO chemisorption results demonstrate that 2Pt/TiP catalyst notably displayed high Pt dispersion and small Pt particle size compared to other catalysts. These results were found to be in agreement with the findings of XRD studies.

3.1.6 Transmission Electron Microscopy (TEM)

TEM images of various metal phosphate supported platinum catalysts presented in Fig. 4 (a–d) show the

Table 2 Physicochemical properties of pure metal phosphates and various metal phosphate supported platinum catalysts

Catalyst	Surface area (m ² /g ⁻¹)	Pore volume (cc/g ⁻¹)	Pore diameter (nm)
Pure AlP	235	1.12	23.6
2Pt/AlP	193	1.03	18.5
Pure TiP	174	0.84	25.1
2Pt/TiP	135	0.35	17.8
Pure ZrP	317	0.13	30.0
2Pt/ZrP	195	0.21	22.9
Pure NbP	189	0.84	23.5
2Pt/NbP	147	0.26	15.2

Table 3 Results of dispersion, CO uptake, metal area, and average particle size of metal phosphate supported platinum catalysts

Catalyst	CO uptake (μmol/g)	Dispersion (%)	Metal surface area (m ² /g) _{cat}	Particle size (nm)
2Pt/AlP	29.8	29.0	1.41	3.8
2Pt/TiP	31.9	31.1	1.51	3.6
2Pt/ZrP	24.2	23.6	1.12	4.7
2Pt/NbP	22.0	21.4	1.02	5.2

morphology and distribution of platinum particles in the catalysts. A homogeneous dispersion of the platinum particles on the surface of metal phosphates was clearly observed and the average size of Pt crystallites was found to be in the range of 4–7 nm.

3.2 Catalytic Performance of the Catalysts

3.2.1 Screening of Metal Phosphate Supported Platinum Catalysts

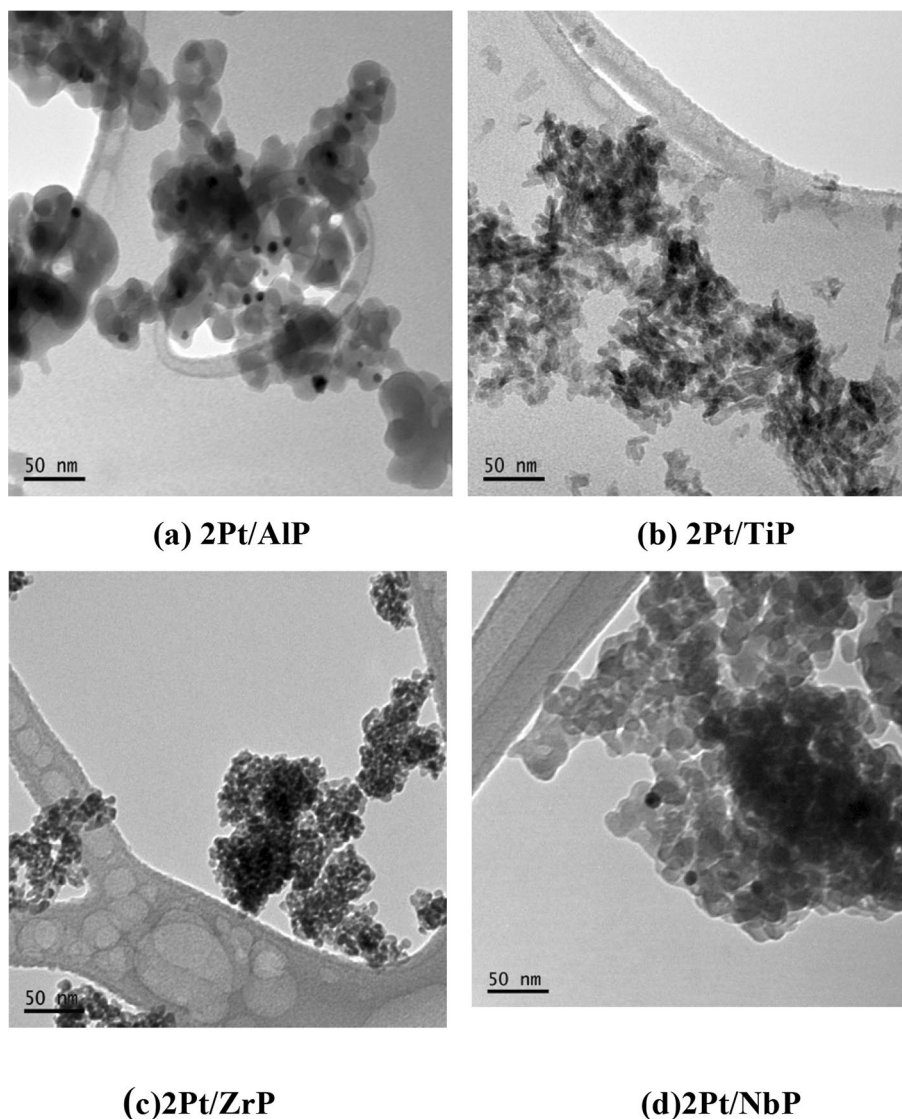
It is well known that hydrogenolysis of glycerol is a complex reaction involving several C–O and C–C cleavage reactions and hence it is essential to monitor the activity and control the selective distribution of products by the use of highly efficient catalytic systems and ambient reaction conditions. In this work, various metal phosphate supported platinum catalysts (2Pt/AlP, 2Pt/TiP, 2Pt/ZrP and 2Pt/NbP) were employed to study its activity towards glycerol hydrogenolysis and examine the product distribution. The reaction of glycerol hydrogenolysis was performed in vapour phase using a continuous fixed-bed reactor under atmospheric pressure. A systematic optimization of the reaction conditions has been carried out to attain the maximum conversion of glycerol and selectivity to products.

We began our studies with the preliminary screening of different metal phosphate supported platinum catalysts for glycerol hydrogenolysis at 220 °C under atmospheric pressure. The comparative results are presented in Table 4. All the metal phosphate supported platinum catalysts exhibited high activity and selectivity towards bio propanols (1-PO + 2-PO) during glycerol hydrogenolysis with appreciable amount of glycerol conversions. In comparison, 2Pt/TiP catalyst showed remarkably high activity among all catalysts reaching a maximum selectivity of 97% to total propanols at full conversion of glycerol. The activity of 2Pt/ZrP and 2Pt/NbP catalysts seems to be high, although the selectivity to propanols was slightly decreased. In contrast, 2Pt/AlP catalyst showed low activity towards the formation of propanols from glycerol but the selectivity to 1,3-PD was comparatively high up to 11%. Except 2Pt/TiP catalyst, all other catalysts were slightly selective to propanediols (1,2-PD & 1,3-PD) besides the formation of 1-PO and 2-PO. The other products identified include acrolein, ethanol, ethylene glycol, methanol and acetone. However, it is interesting to note that, 1-PO was the predominant product of glycerol hydrogenolysis on all metal phosphate supported platinum catalysts.

The formation of acrolein clearly shows that the reaction proceeds in the following way: the dehydration of glycerol over metal phosphates gives acrolein and further hydrogenation over metal sites gives 1-PO, whereas 2-PO is formed by the successive dehydration of glycerol and hydrogenation of acetol. Therefore, based on the results obtained, 2Pt/TiP catalyst was screened out to be the most active and selective catalyst towards the formation of 1-PO & 2-PO during glycerol hydrogenolysis among all other tested catalysts (Scheme 2). The high efficiency of 2Pt/TiP catalyst could be attributed to the presence of strong acidic sites coupled with well dispersed platinum that has facilitated the double dehydration-hydrogenation of glycerol to produce propanols. The strong acidity of 2Pt/TiP catalyst, small particle size and fine dispersion of Pt on TiP support is clearly evident from NH₃-TPD analysis, XRD and CO-chemisorption studies respectively. The catalytic activity results are in good corroboration and well correlate with the characterization results. Therefore, further studies were demonstrated over the most active 2Pt/TiP catalyst to understand the optimized reaction conditions.

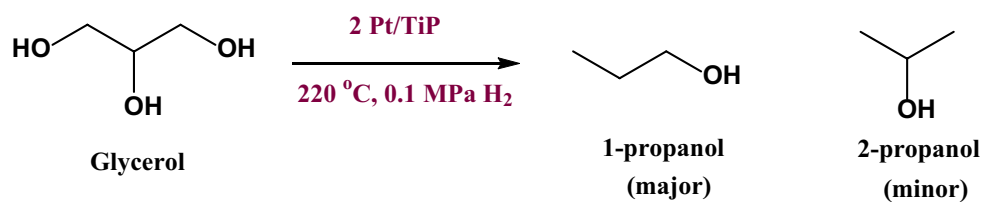
3.2.2 Effect of Platinum Loading

The glycerol hydrogenolysis was performed over a series of Pt/TiP catalysts with varying platinum loading (0.5–3 wt%) in order to understand the impact of platinum loading and find the best performed catalyst. The results of effect of platinum loading on glycerol conversion and selectivity to

Fig. 4 TEM images of various metal phosphate supported platinum catalysts**Table 4** Catalytic performance of various metal phosphate supported platinum catalysts towards glycerol hydrogenolysis

Catalyst	Conversion (%)	Total PO	1-PO	2-PO	1,2-PD	1,3-PD	Acrolein	Others
2Pt/AIP	78	61	38	23	02	11	–	26
2Pt/TiP	100	97	87	10	–	–	02	01
2Pt/ZrP	98	86	68	18	04	1.6	3.3	5.1
2Pt/NbP	90	89	65	24	2.6	2.0	3.0	3.4

Reaction conditions: 0.5 g catalyst; reaction temperature: 220 °C, H₂ flow rate: 100 mL/min; WHSV: 1.02 h⁻¹; 1-PO: 1-propanol, 2-PO: 2-propanol. Others include ethanol, ethylene glycol, hydroxyl acetone, methanol and acetone

Scheme 2 Direct hydrogenolysis of glycerol to propanols

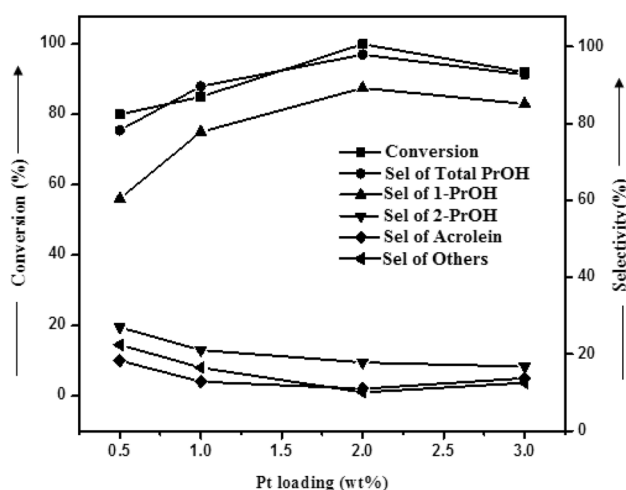


Fig. 5 Effect of Platinum loading on hydrogenolysis of glycerol

products are presented in Fig. 5. It was observed that all the catalysts (0.5–3 wt% Pt/TiP) showed an appreciable activity in glycerol conversion and selectivity to products. On 0.5 Pt/TiP catalyst, 80% glycerol converted with 75.5% selectivity to total propanols. There was a gradual increase in the glycerol conversion as well in the selectivity to propanols (1-PO + 2-PO) when the amount of platinum loaded on the catalyst increased from 0.5 to 2 wt%. The selectivity to 2-PO was found to be maximum at lower loadings and decreased with platinum loading. However, the glycerol conversion and selectivity to propanols slightly decreased on 3Pt/TiP catalyst which is probably due to agglomeration of Pt on TiP, well evident from the characterization results. Therefore, among the series of catalysts (0.5–3Pt/TiP), 2Pt/TiP catalyst was found to be the best catalyst giving maximum conversion and selectivity to total propanols.

3.2.3 Effect of Reaction Temperature

The influence of reaction temperature on glycerol hydrogenolysis over the 2Pt/TiP catalyst as illustrated in Table 5 show that the glycerol conversion greatly improved

from 70 to 100% when the reaction was conducted from 180–260 °C. A complete glycerol conversion was attained at 220 °C and remained stable until 260 °C, while, the selectivity to total propanols gradually increased with rise in reaction temperature, and reached 97% at 220 °C beyond which it decreased. It can be seen that both 1,2-PD and 1,3-PD existed in low selectivity at lower reaction temperatures. Meantime, the selectivity to acrolein gradually decreased when the temperature increased from 180 to 220 °C, indicating that acrolein would have underwent a subsequent hydrogenation reaction over metal sites to form 1-PO. The decrease in the selectivity to 1-PO & 2-PO at higher temperatures indicates the formation of other byproducts such as ethanol, methanol, ethylene glycol and acetone due to excessive C–C cleavage reactions [27]. The maximum glycerol conversion and selectivity to total propanols was obtained at 220 °C reaction temperature.

3.2.4 Effect of Glycerol Concentration

The effect of glycerol concentration on glycerol hydrogenolysis reaction over 2Pt/TiP catalyst at 220 °C was studied by using different concentrations of glycerol (5, 10, 15 &

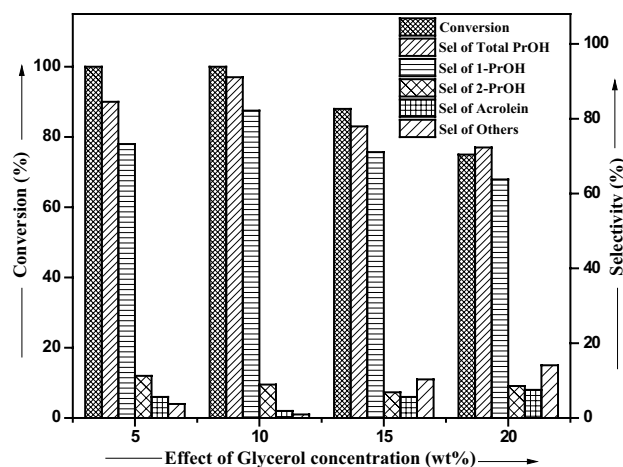


Fig. 6 Effect of glycerol concentration on hydrogenolysis of glycerol

Table 5 Effect of reaction temperature on glycerol hydrogenolysis over 2Pt/TiP catalyst

Reaction Temp (°C)	Conversion (%)	Total PO	1-PO	2-PO	1,2-PD	1,3-PD	Acrolein	Others
180	70	74	59	15	9.0	3.2	9.3	4.5
200	82	80	67	13	5.4	2.2	8.7	3.7
220	100	97	87	10	–	–	02	01
240	100	88	80	08	–	–	4.2	7.8
260	100	84	76	08	–	–	01	15

Reaction conditions: 0.5 g catalyst; reduction temperature: 350 °C, H₂ flow rate: 100 mL/min; WHSV-1.02 h⁻¹; 1-PO: 1-propanol, 2-PO: 2-propanol. Others include ethanol, ethylene glycol, methanol and acetone

20 wt%) and the results are presented in Fig. 6. As anticipated, the glycerol conversion decreased with increase in the amount of glycerol. This observation is obvious because glycerol is a highly viscous liquid and the amount of glycerol fed during the reaction increases at increased glycerol concentration while the number of active sites on the catalyst is constant [28]. Hence there was a decrease in the glycerol conversion from 100 to 75% when the concentration of glycerol is changed from 10 to 20 wt% although remained constant at 5 & 10 wt%. Also, the selectivity to propanols (1-PO+2-PO) was found to be decreased with the formation of undesired byproducts at increased glycerol concentration. It is suggested that 10 wt% glycerol was found to be the optimal concentration resulting in the best performance.

3.2.5 Effect of Hydrogen Flow Rate

It is important to understand the influence of hydrogen flow rate on glycerol conversion and selectivity to products as hydrogen is one of the reactants in the glycerol hydrogenolysis reaction. The reaction was performed over 2Pt/TiP catalyst at 220 °C under atmospheric pressure by varying the rates of hydrogen flow from 60 mL/min to 140 mL/min. As shown in Fig. 7, the glycerol conversion greatly improved from 55 to 100% with increase in the hydrogen flow rate from 60 to 100 mL/min and remained constant with further increase to 140 mL/min hydrogen flow rate. However, there was not much variation in the selectivity of 1-PO & 2-PO although a slight decline was observed at higher flow rates of hydrogen with increase in the degradation products. A similar trend of hydrogen flow rate on glycerol conversion and selectivity was reported in previous studies [29].

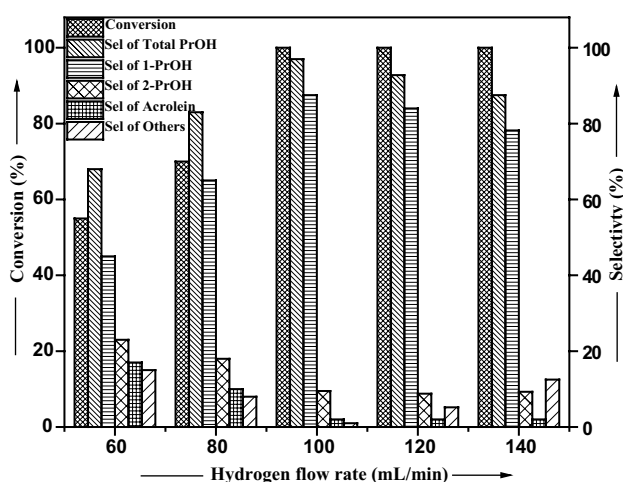


Fig. 7 Effect of hydrogen flowrate on hydrogenolysis of glycerol

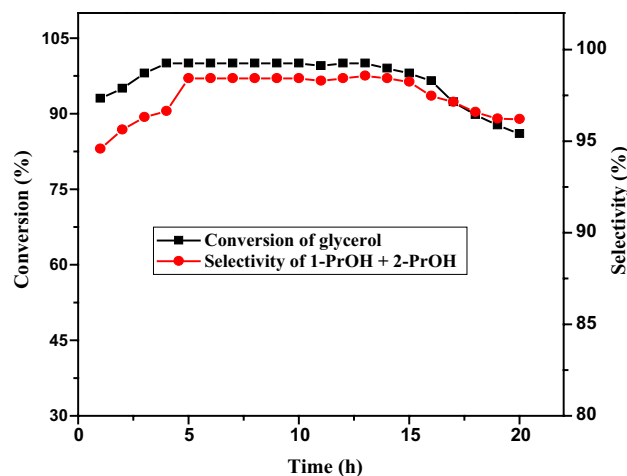


Fig. 8 Effect of reaction time on hydrogenolysis of glycerol

3.2.6 Effect of Reaction Time

The stability of the 2Pt/TiP catalyst has been studied by examining the course of glycerol hydrogenolysis reaction over a period of 20 h at 220 °C and the results are presented in Fig. 8. The catalytic performance of 2Pt/TiP was found to be excellent and remained stable for maximum hours. A complete conversion of glycerol was attained in 4 h and was found to be steady until 13 h after which slightly decreased and reached 86% at the end of 20 h. The similar trend was observed in case of selectivity where it increased from 83 to 97% within a reaction time of 5 h and retained till 14 h. A slow decrease in the selectivity of total propanols (88.9%) was however observed towards the end of 20 h. This behavior of decrease in glycerol conversion and selectivity of propanols is attributed to the catalyst deactivation by coke formation [30]. The time on stream studies suggest the catalyst is quite stable for a long period of time resulting in good catalytic activity during glycerol hydrogenolysis.

3.2.7 Studies on Spent Catalyst

To further confirm the stability of 2Pt/TiP catalyst, the reaction was repeated with spent catalyst (after 1st reaction cycle) under the same reaction conditions. The spent catalyst was characterized to understand the changes that the catalyst has undergone during glycerol hydrogenolysis reaction and the results are shown in Fig. 9 and Table 6. The conversion of glycerol and the selectivity to total propanols (1-PO+2-PO) did not vary significantly over the spent catalyst. There were not much changes observed in the XRD, SEM and TPD patterns of the spent 2Pt/TiP catalyst compared to those of the fresh catalyst as shown in

Fig. 9 XRD and NH₃-TPD patterns of fresh and used 2Pt/TiP catalyst

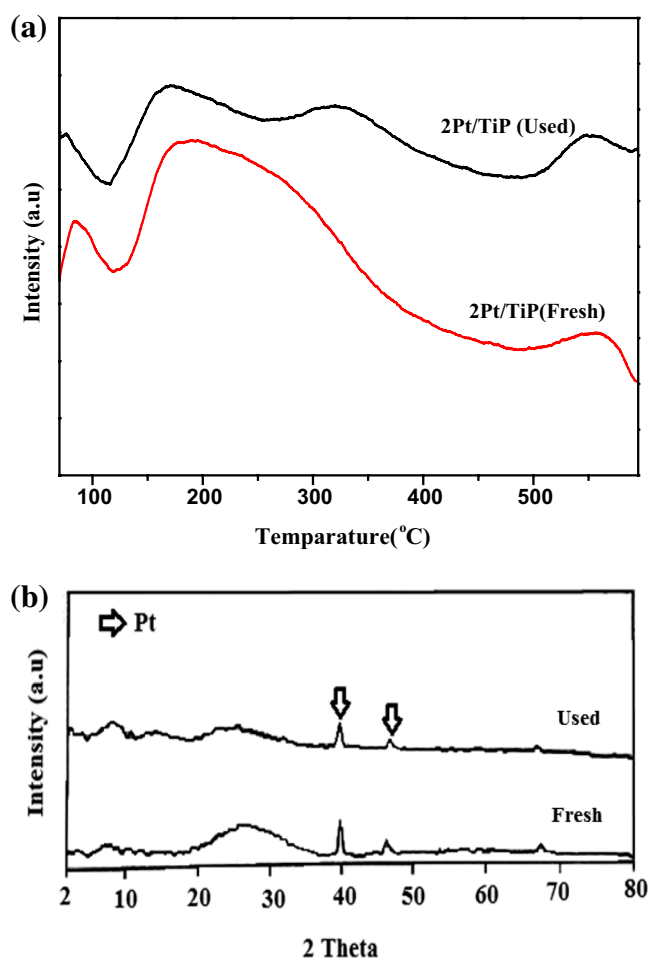


Table 6 Studies of spent catalyst 2Pt/TiP

Catalyst	Conversion (%)	Selectivity of 1-PO + 2-PO	Acidity NH ₃ -TPD (μmol/g)	CHNS analysis (%)			
				C	H	N	S
2Pt/TiP (fresh)	100	97	1123	--	0.3	0.5	--
2Pt/TiP (used)	98	95	1115	1.4	0.3	0.1	--

Fig. 9, which indicates that the structure of 2Pt/TiP catalyst was rather stable during the catalytic reaction.

4 Conclusions

In summary, a sustainable and economic viable one step process of glycerol hydrogenolysis to propanols was described over metal phosphate supported platinum catalysts in vapour phase. It was found that 2Pt/TiP catalyst showed superior performance in glycerol hydrogenolysis with 97% selectivity to total propanols (1-PO + 2-PO) at

complete conversion of glycerol among a series of metal phosphate supported platinum catalysts. The excellent catalytic activity of 2Pt/TiP catalyst is attributed to the strong acidity of the catalyst and well dispersed platinum on the surface of titanium phosphate. The catalyst was found to be quite stable for 20 h reaction time and reusable with a slight decline in the catalytic activity.

Acknowledgements The authors PB and SKH thank University Grants Commission (UGC), New Delhi for the award of Junior Research Fellowship. SSP thanks IICT-RMIT collaboration for the award of fellowship. This work is supported by Indus-Magic program of CSIR network projects under the 12th 5 year plan.

References

1. Zhou CH, Beltramini JN, Fan YX, Lu GQ (2008) *Chem Soc Rev* 37:527–549
2. Soriano MD, Concepción P, López Nieto JM, Cavani F, Guidetti S, Trevisanut C (2011) *Green Chem* 13:2954–2962
3. Rajan PN, Rao GS, Kumar PB, Chary KVR (2014) *RSC Adv* 4:53419–53428
4. Pagliaro M, Ciriminna R, Kimura H, Rossi M, Della Pina C (2007) *Angew Chem Int Ed* 46:4434–4440
5. Priya SS, Kumar VP, Kantam ML, Bhargava SK, Srikanth A, Chary KVR (2015) *Ind Eng Chem Res* 54:9104–9115
6. Priya SS, Bhanuchander P, Kumar VP, Dumbre DK, Periasamy SR, Bhargava SK, Kantam ML, Chary KVR (2016) *ACS Sustainable Chem Eng* 4:1212–1222
7. Zhu MM, Lawman PD, Cameron DC (2002) *Biotechnol Prog* 18:694–699
8. Drent E, Jager WW (2000) US Patent 6:080–898
9. Martin AE, Murphy FH (2000) *Kirk–Othmer encyclopedia of chemical technology*. Wiley, New York, doi:10.1002/0471238961.1618151613011820.a01
10. Priya SS, Bhanuchander P, Kumar VP, Bhargava SK, Chary KVR (2016) *Ind Eng Chem Res* 55:4461–4472
11. Unruh JD, Pearson D (2000) *Kirk–Othmer encyclopedia of chemical technology*, Wiley, New York
12. Logsdon JE, Loke RA (2000) *Kirk–Othmer Encyclopedia of Chemical Technology*. Wiley, New York
13. Zhu S, Zhu Y, Hao S, Zheng H, Mo T, Li Y (2012) *Green Chem* 14:2607–2616
14. Lin X, Lv Y, Xi Y, Qu Y, Phillips DL, Liu C (2014) *Energy Fuels* 28:3345–3351
15. Tamura M, Amada Y, Liu S, Yuan Z, Nakagawa Y, Tomishige K (2014) *J Mol Catal A* 388–389, 177–187
16. Priya SS, Kumar VP, Kantam ML, Bhargava SK, Periasamy S, Chary KVR (2015) *Appl Catal A* 498:88–98
17. Wang M, Yang H, Xie Y, Wu X, Chen, Ma W, Dong Q, Hou Z (2016) *RSC Adv* 6:29769–29778
18. Zhu S, Qiu Y, Zhu Y, Hao S, Zheng H, Li Y (2013) *Catal Today* 212:120–126
19. Priya SS, Kumar VP, Kantam ML, Bhargava SK, Chary KVR (2014) *Catal Lett* 144:2129–2143
20. Priya SS, Kumar VP, Kantam ML, Bhargava SK, Chary KVR (2014) *RSC Adv* 4:51893–51903
21. Fei H, Zhou X, Zhou H, Shen Z, Sun P, Yuan Z, Chen T (2007) *Micro Meso Mater* 100: 139–145
22. Rao GS, Rajan NP, Hari Shekar M, Ammaji S, Chary KVR (2014) *J Mol Catal A* 395:486–493
23. Rao GS, Sowmya M, Rajan NP, Kumar BP, Chary KVR (2014) *App Surf Sci* 309:153–159
24. Dumitriu E, Hulea V (2003) *J Catal* 218:249–257
25. Lercher JA, Gründling C, Eder-Mirth G (1996) *Catal Today* 27:353–376
26. Valente JS, Cantu MS, Cortez JGH, Montiel R, Bokhimi X, Salinas EL (2007), *J Phys Chem C* 111:642–651
27. Wang Y, Zhou J, Guo X (2015) *RSC Adv* 5:74611–74628
28. Kumar VP, Beltramini JN, Priya SS, Srikanth A, Bhanuchander P, Chary KVR (2016) *Appl Petrochem Res* 6:73–87
29. Qin LZ, Song MJ, Chen CL (2010) *Green Chem* 12:1466–1472
30. Kumar VP, Priya SS, Harikrishna Y, Kumar A, Chary KVR (2016) *J Nanosci Nanotechnol* 16:1952–1960